Strong Orbital-Dependent d-Band Hybridization and Fermi-Surface Reconstruction in Metallic $Ca_{2-x}Sr_xRuO_4$

Eunjung Ko,[1] B. J. Kim,[2,*] C. Kim,[1] and Hyoung Joon Choi[1,†]

[1]*Department of Physics and IPAP, Yonsei University, Seoul, 120-749, Korea*

[2]*School of Physics and CSCMR, Seoul National University, Seoul, 151-742, Korea*

(Received 12 October 2006; published 30 May 2007)

We study the effects of RuO_6 rotation on Ru $4d$ band structures in metallic $Ca_{2-x}Sr_xRuO_4$ ($0.5 \leq x \leq 2$) by first-principles electronic structure calculations. We show that the RuO_6 rotation leads to the strong hybridization between d_{xy} and $d_{x^2-y^2}$ bands, resulting in orbital-dependent changes in the band structure. The d_{xy} band near the Fermi level is significantly modified and thereby a severely reconstructed Fermi surface with nested sections appears at $x = 0.5$. In contrast, the d_{yz} and d_{zx} bands are found to be insensitive to the rotational distortions induced by the Ca substitution. Our results imply that the progressive changes in the magnetic, optical, and thermal properties of $Ca_{2-x}Sr_xRuO_4$ are associated with the d_{xy} band.

DOI: 10.1103/PhysRevLett.98.226401 PACS numbers: 71.18.+y, 71.20.−b, 71.30.+h

Orbital-related physics in transition-metal oxides (TMO) have recently attracted much interest in the field of strongly correlated systems [1]. Among $4d$ TMOs, the layered ruthenate $Ca_{2-x}Sr_xRuO_4$ (CSRO) offers a unique challenge as it displays diverse ground states ranging from a superconductor to a Mott insulator [2], rarely found in other $4d$ TMOs. Having four t_{2g} electrons, the orbital degree of freedom in CSRO is of great importance as each d orbital plays a distinct role in different phases. For example, in the superconducting phase ($x = 2$), the d_{xy} orbital of the γ Fermi sheet is known to be the active band responsible for the superconductivity [3], while in the Mott-insulating phase ($x = 0$), electrons are believed to be localized in the $d_{yz,zx}$ orbitals [4,5], possibly with orbital ordering [6].

Of renewed interest in the CSRO system is the anomalous correlated metal phase near $x = 0.5$, which shows critical enhancement of low-temperature susceptibility and strong mass enhancement well inside the range of heavy fermion compounds [7]. It is an interesting problem to determine which orbital is involved in the heavy mass phase and how it is realized. A proposed theory is the orbital-selective Mott transition (OSMT) scenario [5], which predicts coexisting itinerant d_{xy} band and localized $d_{yz,zx}$ orbitals. The results of OSMT are quite interesting, but the studies are based on a model that oversimplifies the effect of the structural distortions. Contrary to the suggested theory, experimental results from neutron scattering [8,9] and optical spectroscopy [10] suggest that the localized spin is associated with the d_{xy} orbital.

As in the work on OSMT, it is widely believed that the electronic ground state in CSRO is tuned by the bandwidth W, via the rotation and tilt of the octahedra induced by the Ca substitution. This has been the usual paradigm for studying metal-insulator transitions (MIT) in $3d$ TMOs with narrow bands which are classified as "bandwidth-controlled systems." However, a recent study on the neighboring $4d$ compound Sr_2RhO_4 [11] showed that this may not be the case for $4d$ TMOs. In Sr_2RhO_4, it is shown that the rotation of octahedra severely modifies the electronic band structures in an orbital-dependent way to the extent that the rotational effect cannot be described by a single parameter W. The most important factor that gives the orbital-dependent changes in the electronic structure was found to be the hybridization between t_{2g} and e_g bands; e_g bands in $4d$ TMOs disperse widely across the crystal field splitting and they overlap with the t_{2g} bands. The possible role of the t_{2g}-e_g hybridization has not been noted in earlier studies of CSRO, although it may have been automatically included in the previous electronic structure calculations [4].

In this Letter, we present electronic structure calculations of metallic CSRO ($0.5 \leq x \leq 2$) by an *ab initio* pseudopotential method based on the local density approximation (LDA). We address specifically the effect of the RuO_6 octahedra rotation and show that it leads to strong hybridization between in-plane orbitals of t_{2g} and e_g bands, resulting in deformation of the d_{xy} band and thus a severe reconstruction of the γ sheet of the Fermi surface. On the other hand, the out-of-plane $d_{yz,zx}$ orbital bands remain essentially intact, the only change being in the occupation number of electrons. We show that CSRO is not a bandwidth-controlled system in the traditional sense as is widely believed, but its bandwidths are altered by the t_{2g}-e_g hybridization in an orbital-dependent way. The resulting γ Fermi surface at $x = 0.5$ consists largely of nested sections, which may explain the observed mass enhancement in the d_{xy} band.

We performed first-principles electronic structure calculations based on the LDA functional and *ab initio* norm-conserving pseudopotentials [12,13] using the SIESTA code [14]. LDA treatment of ruthenates is validated in Refs. [4,15]. A semicore pseudopotential of Ru is generated using an ionic configuration of $4s^2 4p^6 4d^7 5s^0$, with $4s$,

 © 2007 The American Physical Society

$4p$, and $4d$ electrons as valence electrons [16]. Electronic wave functions are expanded with localized pseudoatomic orbitals (double-zeta polarization basis set), and the cutoff energy for the real space grid is 350 Ry. The k-point sampling in the Brillouin zone is made dense enough for good convergence of the total energy.

Sr_2RuO_4 has K_2NiF_4 structure with $I4/mmm$ symmetry. Structural parameters are calculated with the total-energy minimization and then they are used for electronic structure calculations. The calculated parameters are $a = 3.81$ Å and $c = 12.77$ Å with 1.91 Å for in-plane Ru–O distance and 2.07 Å for apical Ru–O. These values are in good agreement with corresponding experimental ones: 3.87, 12.74, 1.93, and 2.06 Å [17], respectively.

$Ca_{1.5}Sr_{0.5}RuO_4$ has lower $I4_1/acd$ symmetry due to in-plane RuO_6 rotation of 12.8° [18], where the Ru–O bond lengths are almost the same as in Sr_2RuO_4. Electronic structures of $Ca_{2-x}Sr_xRuO_4$ are studied using distorted Sr_2RuO_4 which is generated by introducing in-plane RuO_6 rotation of angle θ in a $\sqrt{2} \times \sqrt{2} \times 2$ supercell. The lattice constant $\sqrt{2}a$ is rescaled by $\cos\theta$ to make the Ru–O bond length unchanged, while the lattice constant $2c$ is fixed at 25.54 Å. In the present work, we consider two rotational angles, $\theta = 6°$ and $\theta = 12.8°$, corresponding to $x \simeq 1.2$ and $x = 0.5$, respectively [19].

In Fig. 1(a), we reproduce the well-established band structure of Sr_2RuO_4 [20–22], starting from which we investigate the evolution of the band structure as a function of the Ca content, or equivalently the RuO_6 rotation. In Sr_2RuO_4, three t_{2g} bands cross the Fermi energy (E_F) while two e_g bands are above E_F. The t_{2g} and e_g bands are roughly separated in energy by the crystal field splitting $10Dq$ of ~3 eV [23], which is characteristically large for $4d$ TMOs. However, as the bandwidths are even larger, the $d_{x^2-y^2}$ band disperses down close to E_F at Γ (~0.33 eV), making a negative indirect gap between the t_{2g} and e_g bands [Fig. 1(a)]. The $d_{x^2-y^2}$ band comes to overlap with the t_{2g} bands directly, as shown in Fig. 1(b), in the folded band structure of the $\sqrt{2} \times \sqrt{2} \times 2$ supercell corresponding to the enlarged unit cell in the $I4_1/acd$ symmetry. This suggests that a t_{2g}-e_g scattering with nonzero wave vectors, $q_x = \pm\frac{\pi}{a}$ and $q_y = \pm\frac{\pi}{a}$, may result in significant t_{2g}-e_g hybridization even if the local crystal field splitting is strong inside each RuO_6 octahedron.

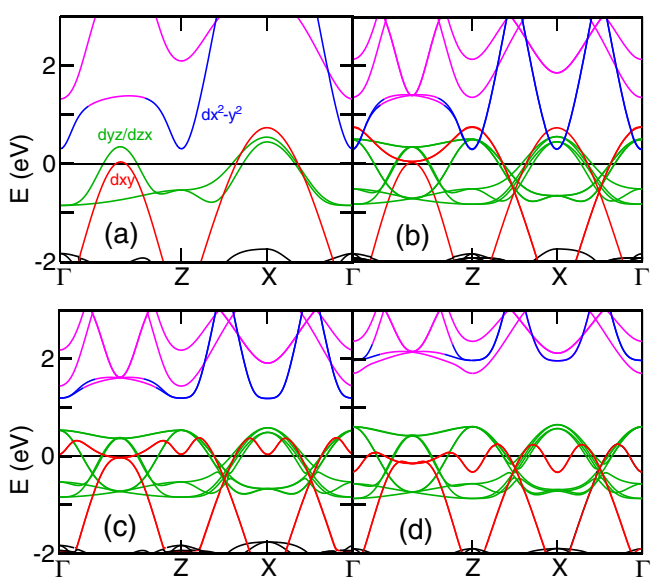

FIG. 1 (color online). Calculated band structures for (a) Sr_2RuO_4 using the primitive unit cell, (b) using the $\sqrt{2} \times \sqrt{2} \times 2$ supercell, and for (c) the 6° and (d) the 12.8° rotation. For comparison, (b)–(d) are plotted at wave vectors corresponding to the high symmetry lines of (a). Bands are color coded. Fermi energy is set to zero. The d_{xy} bandwidth at Γ is 3.85, 3.02, and 2.29 eV for (b), (c), and (d), respectively. The upper part of the d_{xy} bands is strongly modified in (c) and (d), while their lower part is simply rescaled by a factor of $\cos(2\theta)$ [24].

The band structures for $\theta = 6°$ and 12.8°, plotted, respectively, in Figs. 1(c) and 1(d), show the *orbital-dependent* changes upon rotation. The d_{xy} band is severely modified by its hybridization with the $d_{x^2-y^2}$ band, while the $d_{yz,zx}$ bands remain intact apart from a slight upward shift in energy. The hybridization is caused by the intersite d_{xy}-$d_{x^2-y^2}$ scattering with $q_x = \pm\frac{\pi}{a}$ and $q_y = \pm\frac{\pi}{a}$, and its effect is enhanced greatly because of the energy overlap between the unperturbed bands. At $\theta = 12.8°$, the d_{xy} bandwidth at Γ is reduced by as much as 40%, while rescaling of the hopping matrix elements alone would result in only 10% reduction [24]. The narrowing and downward shift of the d_{xy} band was reported previously by Fang and Terakura [4], but its mechanism was not recognized. Our present study shows that the narrowing and downward shift of the d_{xy} band is not simply due to the change in the hopping matrix element as in the traditional bandwidth-controlled systems, but it is caused mainly by the orbital-dependent t_{2g}-e_g hybridization effect. As a result, a gap forms between the otherwise overlapping d_{xy} and $d_{x^2-y^2}$ bands, which pushes down the d_{xy} band and leads to systematic transfer of electrons from the $d_{yz,zx}$ band to the d_{xy} band. The dramatic changes are induced only in the d_{xy} band, which strongly suggests that the progressive changes in the effective mass and the magnetic properties induced by the rotation of octahedra are due to the d_{xy} electrons. Another interesting feature is that at $\theta = 6°$, the van Hove singularity (vHS) point at M, widely discussed in relation to the superconductivity [22], moves below E_F contributing to a large density of states at E_F. At $\theta = 12.8°$, the d_{xy} band is shifted downward further, resulting in an additional d_{xy} Fermi-surface sheet around Γ. This point will be discussed in detail later with Fig. 4(d).

We show in Fig. 2 the calculated projected density of states (PDOS), where the coordinates for the d orbitals are set up locally in the rotated octahedra. Again, this shows the narrowing of the d_{xy} band and essentially unchanged $d_{yz,zx}$ bands. A peculiar aspect of this narrowing is that only

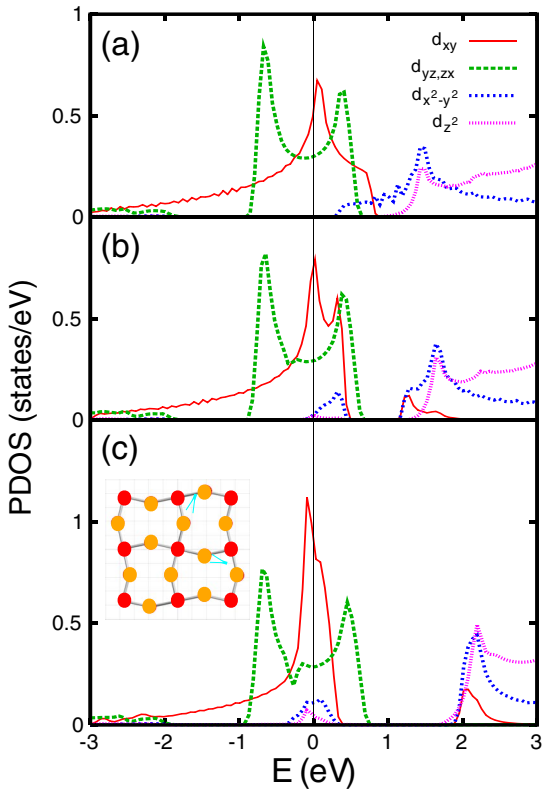

FIG. 2 (color online). Projected density of states (PDOS) near E_F for (a) 0°, (b) 6°, and (c) 12.8° rotations. The inset shows a RuO_2 plane for the 12.8° case and the locally defined x, y axes for PDOS. Red (dark gray) [orange (light gray)] dots are Ru [O] atoms.

the upper part of the d_{xy} band near and above E_F is largely affected, while the low energy part remains almost unaltered. An interesting question is whether this type of narrowing can induce the MIT. In a traditional bandwidth-controlled system, as the bandwidth is narrowed, the gain in the Coulomb energy U by localizing the carriers becomes larger than the gain in the hopping energy t, and thereby the MIT is induced. However, in our case, the bandwidth does not directly reflect the hopping element t and the term "bandwidth narrowing" in the traditional sense may not be appropriate. Nevertheless, some typical features following the bandwidth narrowing can be seen in the PDOS. One can see the PDOS enhancement at E_F at $\theta = 6°$, which is due to the shift of the vHS point just below E_F. It is interesting that just by the rotation of octahedra, the d_{xy} band is "doped" to the level that the vHS point sinks down below E_F. The further enhancement of the PDOS at E_F at 12.8° is due to the formation of an additional d_{xy} Fermi sheet. The enhancement of the PDOS at E_F is consistent with the observed mass enhancement and the increased ferromagnetic correlations implied by the magnetic susceptibility data [7]. However, it cannot account for the strong temperature dependence of the magnetic susceptibility at $x = 0.5$, and the factor by which the PDOS is enhanced is too small to account for the observed mass enhancement. Nonetheless, as will be shown later, the severely reconstructed Fermi-surface topology hints at the origin of these effects.

Figure 3 shows the squared amplitudes of the wave functions on the RuO_2 plane at particular k points for $\theta = 0°$ and 12.8°. In the undistorted case shown in Fig. 3(a) [Fig. 3(b)], the squared amplitude of the $d_{xy}(d_{x^2-y^2})$ band at $X(\Gamma)$ reflects its typical orbital character: the nodal lines (the lobes) of the $d_{xy}(d_{x^2-y^2})$ orbitals point directly to the oxygen ions. As the octahedra are rotated, the two bands are hybridized. Figures 3(c) and 3(d) show that the nominally d_{xy} band and the $d_{x^2-y^2}$ band are actually half-and-half mixtures of locally defined d_{xy} and $d_{x^2-y^2}$ orbitals, as can be inferred from the feature that none of the nodal lines and the lobes point directly to the oxygen ions. Evidence for the hybridization can also be found in Fig. 2(c), which shows the $d_{x^2-y^2}$ PDOS below E_F. This *orbital* occupance of $d_{x^2-y^2}$ may be unfavorable in terms of lattice stability because of the large Jahn-Teller energy of the $d_{x^2-y^2}$ state associated with the elongation of the octahedra. This fact is consistent with the experimental observation of tilting and eventual flattening of the octahedra as x is decreased below 0.5 [2].

The most striking consequence of the hybridization of t_{2g} and e_g bands is the dramatic change in the Fermi-surface topology, as shown in Fig. 4. At the 6° rotation, the γ sheet turns from electronlike to holelike as the vHS point at M sinks below E_F [Fig. 4(c)]. At 12.8° ($x = 0.5$), an additional electronlike Fermi sheet develops around Γ [Fig. 4(d)]. A more interesting feature is that the γ sheet,

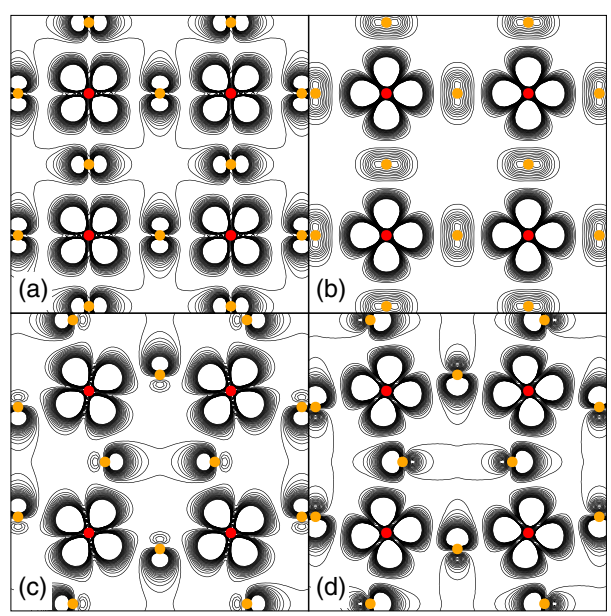

FIG. 3 (color online). Squared amplitudes of the wave functions on a RuO_2 plane: (a) the d_{xy} band at X (0.8 eV above E_F), (b) the $d_{x^2-y^2}$ band at Γ (0.3 eV) for $\theta = 0°$, (c) the d_{xy} band at Γ (-0.3 eV), and (d) the $d_{x^2-y^2}$ band at Γ (2 eV) for $\theta = 12.8°$. Red (dark gray) [orange (light gray)] dots are Ru [O] atoms.

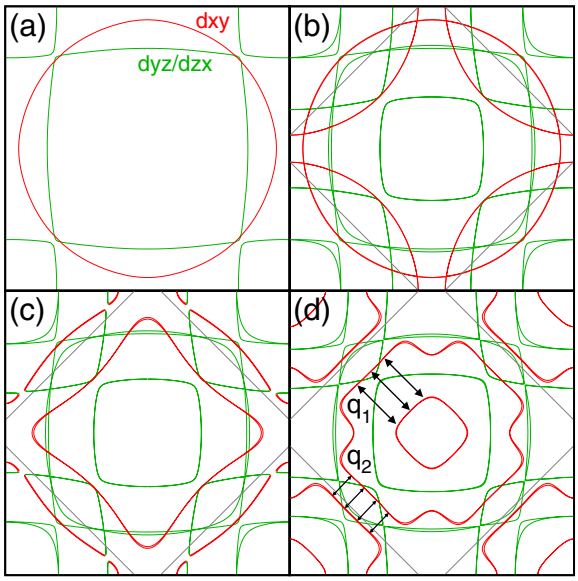

FIG. 4 (color online). Calculated Fermi surfaces for (a) undistorted Sr_2RuO_4 using the primitive unit cell and (b) using the $\sqrt{2} \times \sqrt{2} \times 2$ supercell, (c) $\theta = 6°$ ($x \simeq 1.2$), and (d) 12.8° ($x = 0.5$). The center and four corners of each plot correspond to the Γ and X of undistored Sr_2RuO_4, respectively. The gray lines represent the Brillouin zone of the supercell.

which had a circular shape, now consists of mostly straight sections connected to each other by **q** vectors as marked by arrows in Fig. 4(d). This suggests the anomalies at $x = 0.5$ are related to the nesting instabilities. A universal observation in a wide variety of layered TMOs with nested Fermi surfaces is the destruction of coherent transport of the carriers. Examples include high-T_c superconductor $Ca_{2-x}Na_xCuO_2Cl_2$ [25] and colossal-magnetoresistive material $La_{1.8}Sr_{1.2}Mn_2O_7$ [26,27], in which quasiparticles are destructed possibly by static or dynamic spin or charge density waves. The same behavior is also observed in a sister compound $Ca_3Ru_2O_7$ [28], in which metallic pockets are found only in the non-nested sections. This apparent universality in the compounds with similar layered structures strongly points towards the possibility that the anomalies at $x = 0.5$ stem from its nested Fermi surface. We suggest further study to uncover the possible existence of instability at $\mathbf{q}_1 \approx (\pm\frac{2\pi}{7a}, \pm\frac{2\pi}{7a}, 0)$ and $\mathbf{q}_2 \approx \frac{1}{2}\mathbf{q}_1$.

In summary, our results indicate that significant changes are induced by the rotation of the octahedra in the band structures and thereby the Fermi-surface topology of the d_{xy} band. They are fully consistent with the topological change of the γ sheet observed at the $\sqrt{2} \times \sqrt{2}$ reconstructed surface of Sr_2RuO_4 [20], the absence of the γ sheet in Sr_2RhO_4 [11], and in some aspect to the recent angle-resolved photoemission spectroscopy result on $Ca_{1.5}Sr_{0.5}RuO_4$ [29,30]. The results also naturally account for the experimental observation that the mass enhancement occurs in the d_{xy} band. All of these phenomena stem from the hybridization of t_{2g} and e_g bands, which is a robust mechanism that affects the electronic band structure of 4d TMOs.

This work is supported (in part) by Yonsei University Research Fund of 2005 and by the core capability enhancement program of KIST, "Massive Scientific Calculation Technology for Modelling of Nano Process and Devices." B. J. K. and C. K. are supported (in part) by the KOSEF through the CSCMR. C. K. acknowledges support by MOST through the Global Partnership Program. Computational resource is provided by KISTI under the 7th Strategic Supercomputing Support Program.

*Electronic address: bjkim6@gmail.com
†Electronic address: h.j.choi@yonsei.ac.kr

[1] Y. Tokura and N. Nagaosa, Science **288**, 462 (2000).
[2] S. Nakatsuji and Y. Maeno, Phys. Rev. Lett. **84**, 2666 (2000); Phys. Rev. B **62**, 6458 (2000).
[3] Y. Maeno, T. M. Rice, and M. Sigrist, Phys. Today **54**, No. 1, 42 (2001).
[4] Z. Fang and K. Terakura, Phys. Rev. B **64**, 020509 (2001); Z. Fang, N. Nagaosa, and K. Terakura, Phys. Rev. B **69**, 045116 (2004).
[5] V. I. Anisimov *et al.*, Eur. Phys. J. B **25**, 191 (2002).
[6] T. Hotta and E. Dagotto, Phys. Rev. Lett. **88**, 017201 (2001).
[7] S. Nakatsuji *et al.*, Phys. Rev. Lett. **90**, 137202 (2003).
[8] A. Gukasov *et al.*, Phys. Rev. Lett. **89**, 087202, (2002).
[9] O. Friedt *et al.*, Phys. Rev. Lett. **93**, 147404 (2004).
[10] J. S. Lee *et al.*, Phys. Rev. Lett. **96**, 057401 (2006).
[11] B. J. Kim *et al.*, Phys. Rev. Lett. **97**, 106401 (2006).
[12] M. L. Cohen, Phys. Scr. **T1**, 5 (1982).
[13] N. Troullier and J. L. Martins, Phys. Rev. B **43**, 1993 (1991).
[14] D. Sánchez-Portal *et al.*, Int. J. Quantum Chem. **65**, 453 (1997).
[15] I. I. Mazin and D. J. Singh, Phys. Rev. Lett. **79**, 733 (1997).
[16] J. Junquera and P. Ghosez, Nature (London) **422**, 506 (2003).
[17] Y. Maeno *et al.*, Nature (London) **372**, 532 (1994).
[18] O. Friedt *et al.*, Phys. Rev. B **63**, 174432 (2001).
[19] The 6° rotation is assigned to $x \simeq 1.2$ by linear interpolation between 0° for $x = 1.5$ and 10.8° for $x = 1.0$ [18].
[20] A. Damascelli *et al.*, Phys. Rev. Lett. **85**, 5194 (2000).
[21] T. Oguchi, Phys. Rev. B **51**, 1385 (1995).
[22] D. J. Singh, Phys. Rev. B **52**, 1358 (1995).
[23] H.-J. Noh *et al.*, Phys. Rev. B **72**, 052411 (2005).
[24] In our result, Ru–O hopping matrix elements ($pd\sigma$, $pd\pi$) are almost independent of θ since Ru–O bond lengths are unchanged. Meanwhile, the bending of the Ru–O–Ru bonds rescales effective hopping matrix elements between d_{xy} orbitals by $\cos(2\theta)$, which is 0.9 for $\theta = 12.8°$.
[25] K. M. Shen *et al.*, Science **307**, 901 (2005).
[26] Y.-D. Chuang *et al.*, Science **292**, 1509 (2001).
[27] N. Mannella *et al.*, Nature (London) **438**, 474 (2005).
[28] F. Baumberger *et al.*, Phys. Rev. Lett. **96**, 107601 (2006).
[29] S.-C. Wang *et al.*, Phys. Rev. Lett. **93**, 177007 (2004).
[30] Our calculated Fermi surface is consistent with the one measured by S.-C. Wang *et al.* in that the γ bands turn holelike. However, we argue that it necessarily accompanies the transfer of electrons among the t_{2g} bands, contrary to their claim that there is no charge transfer.